Chapter 6

Development of an affordable transradial prosthesis based on force myography

6.1 Introduction

More than 60% of the upper-limb amputees worldwide are transradial (i.e., below elbow amputation). Trauma, cancerous tumor in muscles and bones, vascular disease, infection, etc., are the chief causes responsible for such amputations (Maduri and Akhondi 2020; Fahrenkopf et al. 2018). Moreover, the majority population of upper-limb amputees is reported from the countryside. The currently available hand prostheses can reinstate the amputee's lost functionality, but their overall cost is too high. The survey report tells that more than 85% of transradial amputees cannot afford functional prosthetic devices (Hamner, Narayan, and Donaldson 2013; Slade et al. 2015; "World Report on Disability," 2011). Body-powered and cosmetics prostheses are still used by most patients who are incapable of fulfilling their needs of daily life (Kannenberg 2017; Uellendahl 2017). The amputee community needs an artificial hand that is functional, affordable, and also easy to operate.

Myoelectric prosthesis utilizes EMG signals from the residual upper-limb of patients to operate the terminal device, using a suitable control strategy (Parker, Englehart, and Hudgins 2006; Asghari Oskoei and Hu 2007). These days such prosthesis has become extensively accessible in the market because EMG signals are easy to acquire, and these are also capable of providing user-intention based control to the device (Tavakoli, Benussi, and Lourenco 2017; Pancholi and Joshi 2018). Bebionic v3, i-limb quantum, vincent evolution 3, and michelangelo are some commercial myoelectric hands that can provide numerous grip patterns to precisely grasp distinct shaped objects. These full-featured hands can accomplish activities of daily livings (ADLs), but their price is exceptionally high("Bebionic Hand"; "I-Limb Quantum | Touch Bionics"; "VINCENTevolution 3"; "Michelangelo Prosthetic Hand"). Moreover, these are

based on a complicated control scheme that requires a large number of training sessions for their reliable function (Wang, Oskoei, and Hu 2017).

Besides having advantages, the EMG technique also has some limitations, which are: (1) It requires complex preprocessing circuitry and electrodes in direct, as well as steady electrical interaction with skin (2) the EMG signals are prone to sweat, humidity, electrode shift, motion artifact, crosstalk, and other electrical interference (3) electrode performance, deteriorates with time (4) the signal patterns shows unsteadiness with time (Connan et al. 2016; Abdoli-Eramaki et al. 2012; Castellini et al. 2014; Peerdeman et al. 2011). These issues significantly influence the ability of EMG to control the prosthetic device.

Force myography (FMG) is another technique to detect the activity of muscles like EMG. FMG measures the mechanical variations that occur during muscle contraction. During muscular contraction, the parameters like muscle volume and stiffness change, which produces forces outward. In the FMG technique, force sensing elements are used to register the changes in muscle volume during contraction (Ibitoye et al. 2014; Cho et al. 2016). Compared to EMG, FMG is low-cost, effortless, and insusceptible to electrical noise and does not necessitate the use of electrodes and sophisticated conditioning circuitry. It also yields a quite repeatable and steady output as a function of time compared to EMG (Connan et al. 2016; Radmand, Scheme, and Englehart 2016). FMG can extract detailed information about the muscular contractions that can be effectively applied for controlling prostheses and other assistive devices. In recent days, the application of FMG signal as a source to control prosthetics has gained much attention (Ha, Withanachchi, and Yihun 2018).

A comparison was made between EMG and FMG for applying the human-machine interface. It was found that FMG provides improved control because of its skill to give top classification

accuracy, signal stability over time, affordable system, etc. (Ravindra and Castellini 2014). Closing and opening of a prosthetic hand were performed using signals from 32 pressure sensors attached to the residual upper-limb of the amputee by placing it between the socket and the skin interface (Phillips and Craelius 2005). A group of force sensors was utilized for accomplishing classification-based control of the prosthetic hand (Xiao and Menon 2014). Using FMG data, linear discriminant analysis (LDA), support vector machine (SVM), and extreme learning machine (ELM) based classification were done for the offline and real-time control of hand prosthesis (Ahsan, Ibrahimy, and Khalifa 2011). Various hand activities were captured and classified for hand prosthesis control, using a piezoresistive array sensor worn around the forearm (Ha, Withanachchi, and Yihun 2019).

Hand prosthesis based on FMG has a potential for carrying out activities of daily livings (ADLs) for amputees. However, the utility of such devices is limited to research work only. The foremost reasons are unsteady contact of sensors on the skin surface, uneven transfer of muscular contractile force on the active area of the sensor, signal drift, lack of intuitiveness in control, use of a large number of sensing elements make the system complex, etc. (Esposito et al. 2018a; Lobo-Prat et al. 2014).

This chapter presents a low-cost transradial prosthesis controlled by FMG signal. An FMG sensor was fabricated with exclusive mechanical construction and signal conditioning circuitry, which could faithfully detect the muscle contractions from the remaining upper-limb of amputees. The sensor's performance was authenticated by evaluating its static and dynamic features. Also, its ability to detect muscle activity was compared with that of a standard EMG sensor. A 3D printed prosthetic hand was developed with a proportional based position control system that accepts reference input from the designed sensor. The hand prototype with

specially designed socket assembly was successfully tested on different subjects for performing basic activities of daily life. Amputees wearing the prosthesis in their residual limb were able to grasp different objects by utilizing intention-based muscle contractions dexterously.

6.2 Materials and Methods

6.2.1 Fabrication of sensor

FMG technique utilizes force sensing elements placed on the active area of muscle to measure contraction. A force-sensitive resistor (FSR) is a piezoresistive-based element whose resistance decreases with applied force. Due to its low-cost, good accuracy, small dimension, and lightweight, FSR has frequent applications in FMG. However, placing FSR directly on the skin (in combination with a sensitive muscle) may provide undesired output regarding muscle contraction. Because skin may exert uneven force on the FSR's sensing area, it can also lead to its inappropriate bending (Lukowicz et al. 2006; Junker et al. 2008). An FMG sensor was proposed with a novel mechanical design shown in Figure 6.1(a) to overcome these limitations.

The sensor was designed with an explicit mechanical arrangement consisting of an FSR (FSR-402) embedded inside a 3D printed chassis with a stiff coupler. The FSR's circular sensitive portion was sandwiched between two thin layers of polydimethylsiloxane material (i.e., PDMS layer 1 and layer 2) to support appropriate force distribution by coupler on it. The force sensing tip of the coupler receives the muscular contraction from the skin surface, which is evenly transmitted to the FSR for the production of electrical output. The 3D printed chassis delivers rear support to FSR by averting its unsuitable bending and encourages the application of proper force over its active area. The flexible element in the sensor acts as a dummy sensing tip,

which, along with the active sensing tip, produces a grip with the skin for detecting even the shorter muscle contractions.

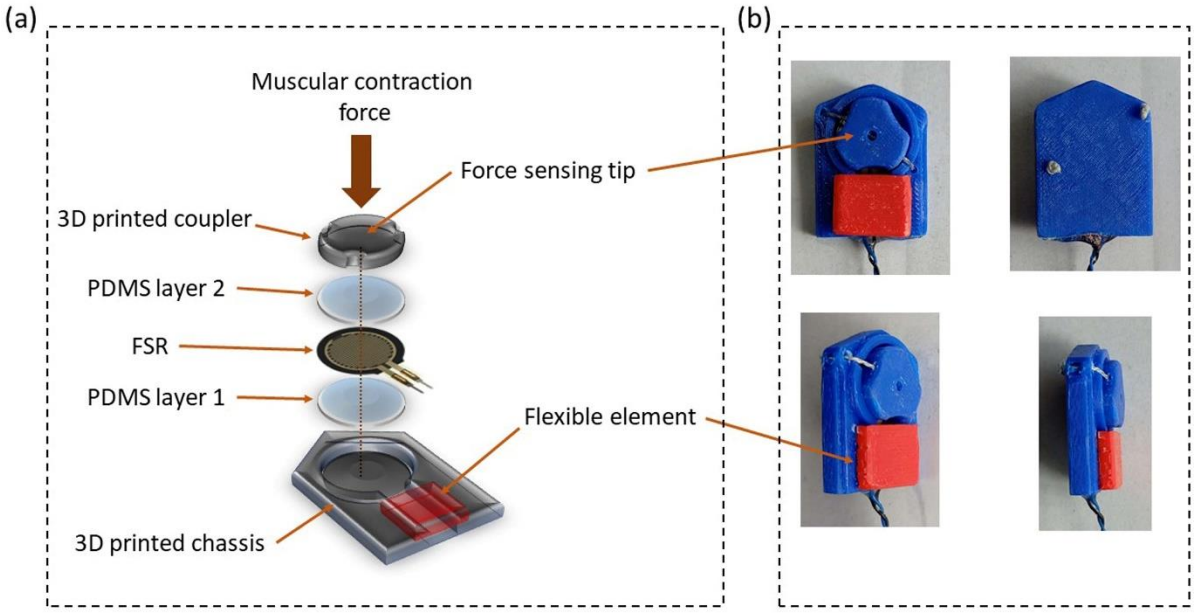

Figure 6.1 (a) Mechanical assembly of the proposed FMG sensor, (b) front, rear, and side views of the designed FMG sensor.

A specific sig FSR generally uses a conventional buffered voltage divider circuitry for converting the change in resistance to the voltage output. However, such a circuit gives a non-linear relationship between the output voltage and the input resistance. These circuits also affect the sensor's static parameters, such as sensitivity, repeatability, and hysteresis (Matute et al. 2018; Amft et al. 2006). A simple transimpedance amplifier shown in Figure 6.2(b) was incorporated as a translating circuitry for the sensor(Paredes-Madrid et al. 2018). Equation (6.1) gives the output (V_{out}) for the circuit where V_{FSR} is the input voltage to the FSR, R_{FSR} is the resistance of the FSR and R_F is the feedback resistance.

$$V_{out} = -V_{FSR}\frac{R_F}{R_{FSR}} \tag{6.1}$$

This circuit delivers constant voltage to FSR, which leads to fixed sensitivity of the device for several force inputs. The value of R_F was set at a value of 8 Ω to achieve the required sensitivity for the application. A step-down converter circuit (MP1584 module) shown in Figure 6.2(a) was used to provide a small input voltage V_{FSR} to the transimpedance amplifier.

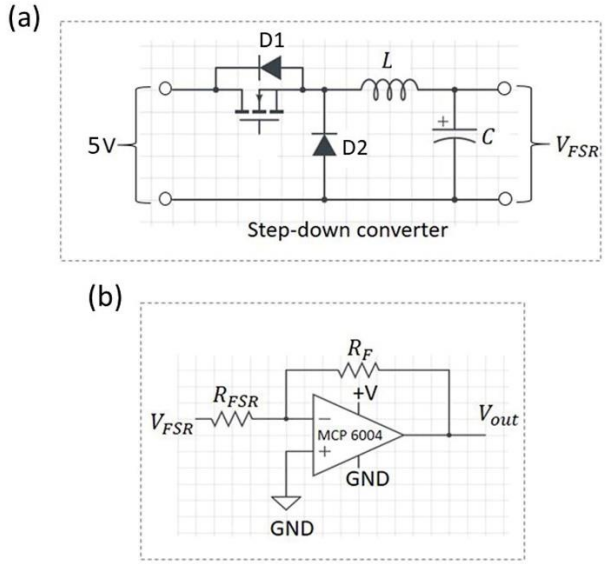

Figure 6.2 (a) Step-down converter circuit, (b) transimpedance amplifier.

Figure 6.1(b) shows the different views of the designed sensor. The sensor's dimension was 2 cm x 3 cm. The sensor can be easily attached to the subject's forearm through a velcro strap for measuring muscle contractions. The conditioning circuitry of the sensor produces output voltage as a 0-5 V linear envelope proportional to the intensity of muscular contraction.

6.2.2 Sensor validation

The different static and dynamic characteristics of the sensor, like sensitivity, repeatability, hysteresis, and frequency response, were determined to analyze its force detecting performance.

6.2.2.1 Sensitivity

An experiment was done in which various weights were placed vertically on the force-sensing tip of the sensor one after another, and output voltages were acquired. A calibration curve between input weight and the output voltage was obtained in which the slope of the curve gives the sensor's sensitivity.

6.2.2.2 Repeatability

Repeatability of the FMG sensor provides its ability to produce the same output voltage for repeated application of the same input force under similar measurement conditions. For five repetitive applications of the same weight on the sensor tip, the repeatability error was determined as the relative standard deviation (RSD) using equation (2) (Esposito et al. 2018b). The error was calculated for all eleven weights.

$$RSD = \frac{\sqrt{((X-\bar{X}))/n}}{\bar{X}} \times 100 \quad (6.2)$$

Where $\bar{X}$ is the mean value of data samples, X is any value in the data samples, and n is the number of samples.

6.2.2.3 Hysteresis

A hysteresis error curve was obtained for the sensor for change in voltage output with increment and decrement in input load (i.e., for increasing and decreasing order of applied weight).

6.2.2.4 Frequency response

Dynamic characteristic, i.e., the sensor's frequency response, was evaluated to know its capability in detecting dynamic contractions (i.e., rapidly changing FMG signals). An experiment was performed in which an electrodynamic shaker (Model: 2007E) was used to

provide a rapidly varying force (i.e., vibration) to the sensing tip of the designed sensor (Esposito et al. 2018b). The shaker also consists of an accelerometer sensor for measuring the vibrations produced by its tip. The shaker was excited with a fixed AC voltage of variable frequency (1-3 kHz) employing a signal generator. The FMG sensor and accelerometer voltage output were simultaneously acquired for each frequency value using a data acquisition (DAQ) device. All the data were acquired at a sampling rate of 2 KS/s. The actual force applied by the shaker was a calibrated version of the voltage produced by the accelerometer because the weight of the accelerometer was fixed. Further, the frequency response gain was calculated as the ratio of force measured by the FMG sensor to the actual force delivered by the shaker.

6.2.2.5 Correlation with EMG signal

Sensor ability in detecting muscular contractions from the forearm muscles of subjects was compared with that of a previously designed EMG sensor. Both the sensors were positioned at flexor carpi radialis muscles on the forearm close to each other, and simultaneous acquisition of FMG and EMG signals was done for three different activities: (1) maximum voluntary contraction (MVC), (2) 50% of MVC, (3) 25% of MVC (Esposito et al. 2018). For quantitatively analyzing the similarity, a two-tailed paired t-test was performed between recorded FMG and EMG signals.

6.2.2.6 SNR calculation

To quantify the noise performance of the designed sensor, signal-to-noise ratio (SNR) was evaluated for both the sensors. The parameter was calculated for the simultaneously acquired FMG and EMG signals from similar muscle locations. It was calculated as the ratio of root mean square (RMS) value of the signal for the maximum voluntary contraction to the RMS

value of baseline noise for no muscle activity(Agostini and Knaflitz 2012). SNR values were determined for both the sensors considering each subject, using equation (6.3).

$$SNR = 20\ log_{10}\left(\frac{RMS_{signal}}{RMS_{noise}}\right) \quad (6.3)$$

6.2.3 Prosthetic hand development

6.2.3.1 3D printing

A hand model parts were custom-designed and were prepared using 3D printing. The printing was carried out using the fused deposition modeling (FDM) technique utilizing polylactic acid (PLA) filament with an extruder temperature set at 220℃ (Melocchi et al. 2015). All the 3D printed parts were assembled to form the hand prototype. Specific socket assembly for the amputee's residual limb was designed and was attached to the hand prototype. Above the socket, a cabinet was intended for the actuator unit. The views of the 3D printed hand prototype are shown in Figure.

6.2.3.2 Actuation

Extrinsic actuation mechanism was executed for the designed hand prototype in which the actuator was situated on the socket assembly, i.e., outside the palm. This scheme provides natural weight dissemination to the hand (Pylatiuk et al. 2004). Motor-tendon based actuation scheme was applied for the flexion of fingers. Such a tactic converts the high torque of the motor to augmented linear flexion force without any speed loss (Williams and Walter 2015). Figure 6.3 shows the basic actuation scheme for the hand fingers. Tendons were responsible for the flexion of fingers through the angular displacement of servomotor (using pulley), whereas the extension of fingers was provided by elastic elements attached to the phalangeal joints. In this actuation scheme, a single digital servomotor (DS-3225) was employed to flex

all the fingers and the thumb. The servomotor with pulse width modulation (PWM) signal as input produces angular displacement in the 0-180^0 range and can provide maximum torque up to 25 kg.f.cm.

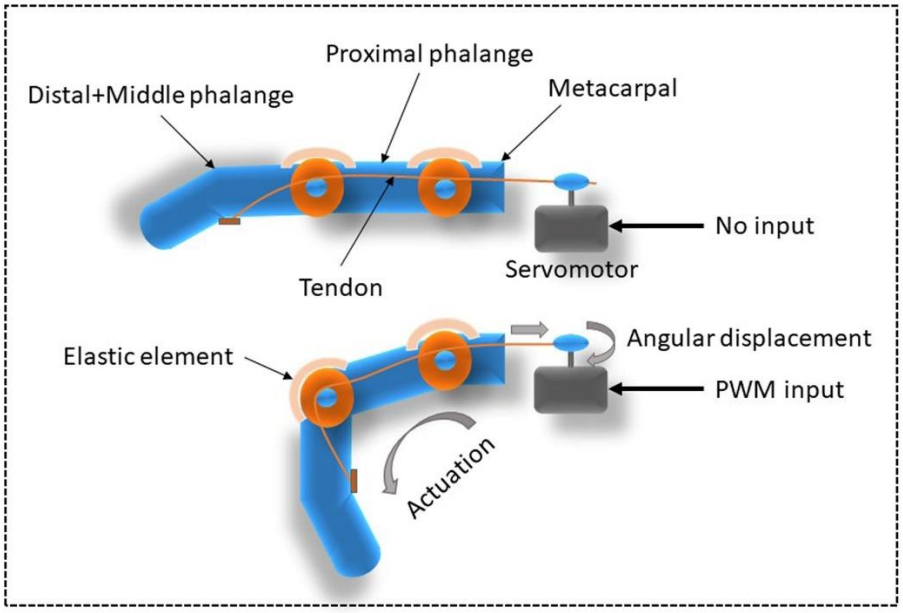

Figure 6.3 Actuation scheme for the hand fingers.

6.3 Results and discussion

6.3.1 Sensitivity

Figure 6.4 shows the obtained calibration curve for the sensor in which dotted points are experimentally measured values, whereas the straight line represents the linear regression. A linear fitting was performed for the plot, which showed Pearson's coefficient (r=0.99) and adjusted coefficient of determination (Adj. r^2=0.99), revealing a good fitting. Further, the sensitivity of the sensor was evaluated as 3.2 V/kg. It was found that the sensitivity of the sensor was almost constant for all ranges of applied weights. This feature allows the sensor to measure the shorter as well as longer muscle contractions reliably.

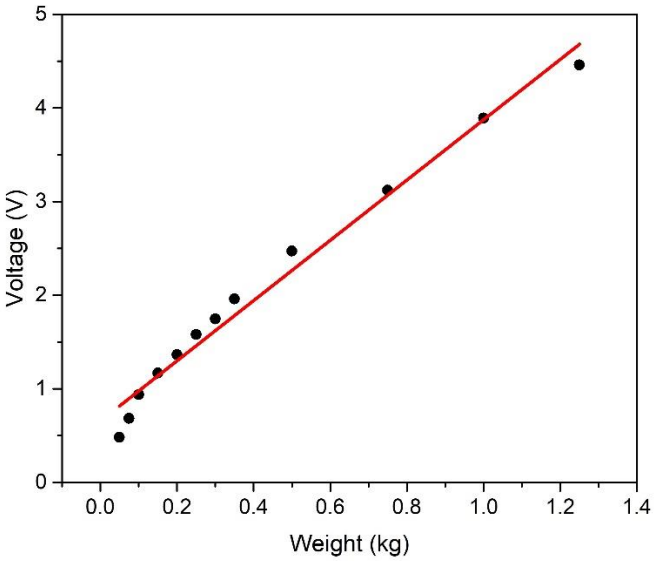

Figure 6.4 Static calibration curve for the sensor.

6.3.2 Repeatability

The box whisker's plot mentioning the repeatability error of the sensor in terms of %RSD for all the applied weights is shown in Fig. 5. The overall repeatability error for the sensor was 1.6%. It is clear from the plot that the sensor is slightly less repeatable for lighter loads. However, as a whole, it can be observed that the sensor has a useful repeatability feature that can be effectively utilized for detecting mechanical muscle contractions.

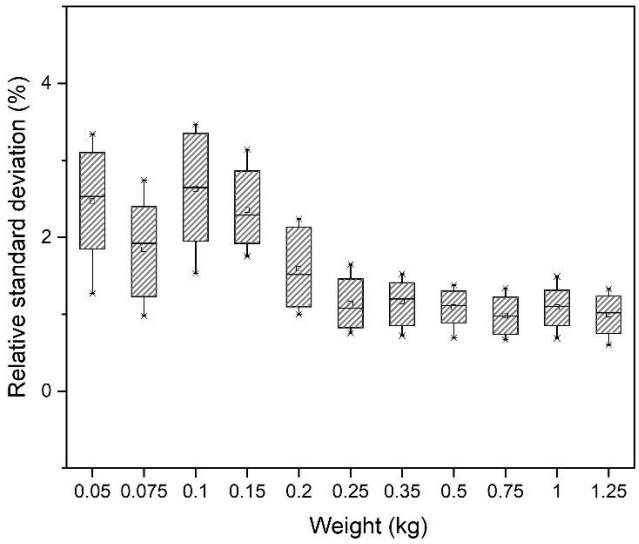

Figure 6.5 Repeatability error curve for the sensor.

6.3.3 Hysteresis

Fig. 6 describes the hysteresis curve obtained for the sensor. The average hysteresis error for the sensor was around 3%, which is very less as compared to a simple FSR (having 10%)("FSR Integration Guide").

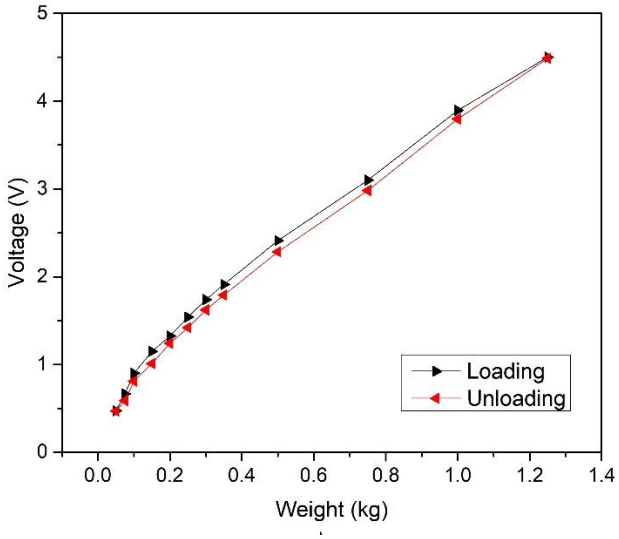

Figure 6.6 Hysteresis curve for the sensor.

6.3.4 Frequency response curve

Figure 6.7 depicts the frequency response curve for the sensor in which a smooth response was observed up to a frequency of 600 Hz. A resonance peak was obtained approximately at 850 Hz, after which the response starts to decay sharply. From these dynamic characteristics, it can be concluded that the designed FMG sensor can detect dynamic contractions in the range of 0-600 Hz.

6.3.5 FMG-EMG correlation

Simultaneously recorded FMG and EMG envelopes for three different muscular contractions of forearm muscles are shown in Fig. 6.8. Conducted paired t-test between these two signals (i.e., FMG and EMG) showed a good correlation coefficient ($r>0.91$ with a p-value<0.0001).

This result revealed that the FMG sensor could be used as an excellent alternative to the EMG sensor.

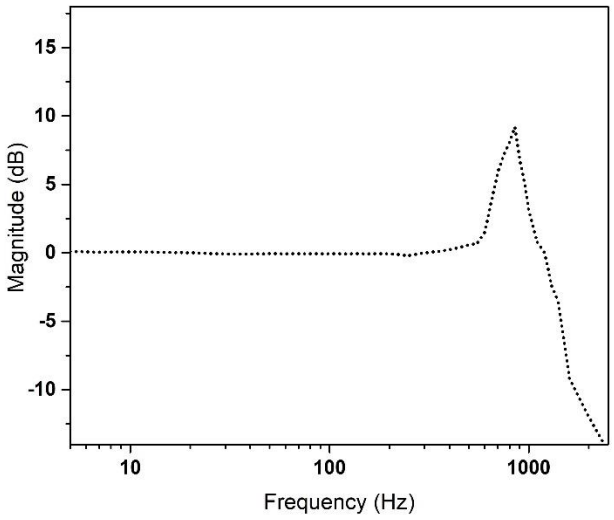

Figure 6.7 The frequency response curve for the sensor.

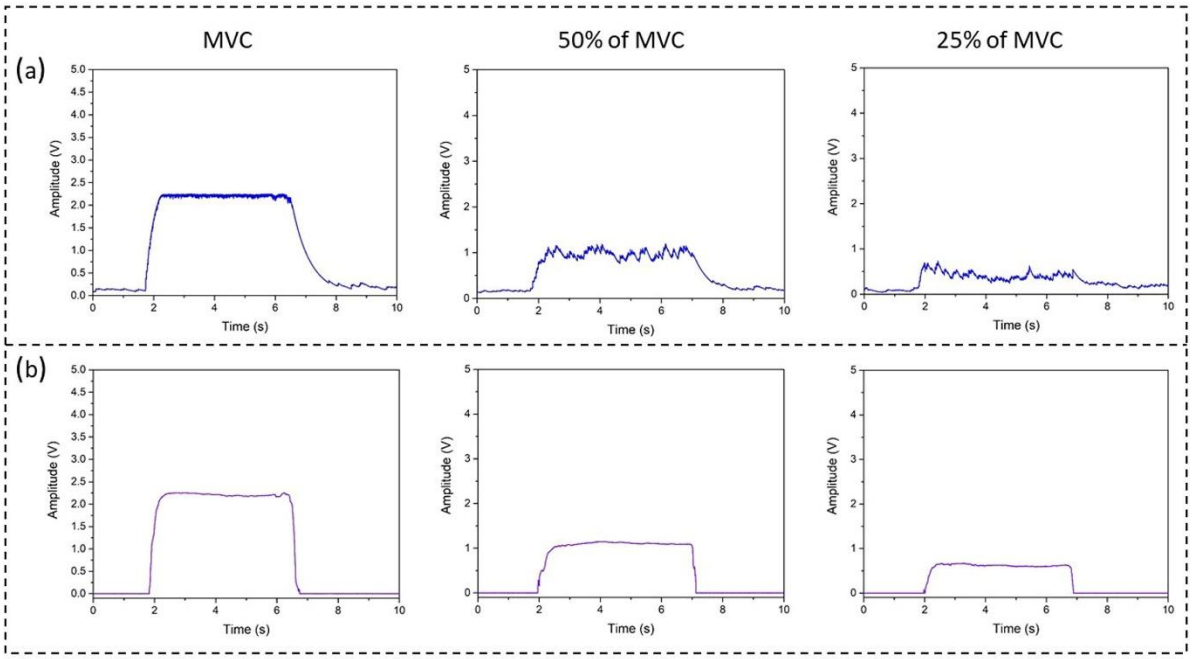

Figure 6.8 Simultaneously acquired FMG and EMG envelopes for MVC, 50% MVC, and 25% MVC.

6.3.6 SNR comparison

Table 6.1 indicates the determined SNR values for both sensors. The designed FMG sensor showed very high SNR values as compared to the EMG sensor. As per the literature SNR parameter decides the quality of EMG signal whose value can lie between 0-50 dB in perfect situations (Sinderby, Lindstrom, and Grassino 1995).

Subjects	**SNR (dB)**	
	Designed sensor	**EMG sensor**
1.	43.7	19.8
2.	43.2	19.2
3.	44.7	20.4
4.	46.3	22.6
5.	44.9	21.5
6.	45.1	21.9
7.	45.3	22.1
8.	44.2	20.2
9.	44.8	20.7
10.	46.5	22.8
Average	44.8	21.1

Table 6.1 Evaluated SNR for both the sensors.

6.4 Hand prosthesis control

6.4.1 Control scheme

A proportional based position control scheme shown in Figure 6.9 was incorporated to actuate the developed hand prototype using input FMG signal. The mechanical muscle contraction detected by the sensor in 0-5 V was calibrated to control the duty cycle of the PWM signal

proportionally for driving the servomotor. The angular displacement produced by the servomotor was used to actuate the hand fingers accordingly. An algorithm for this scheme was formulated and burned to a microcontroller.

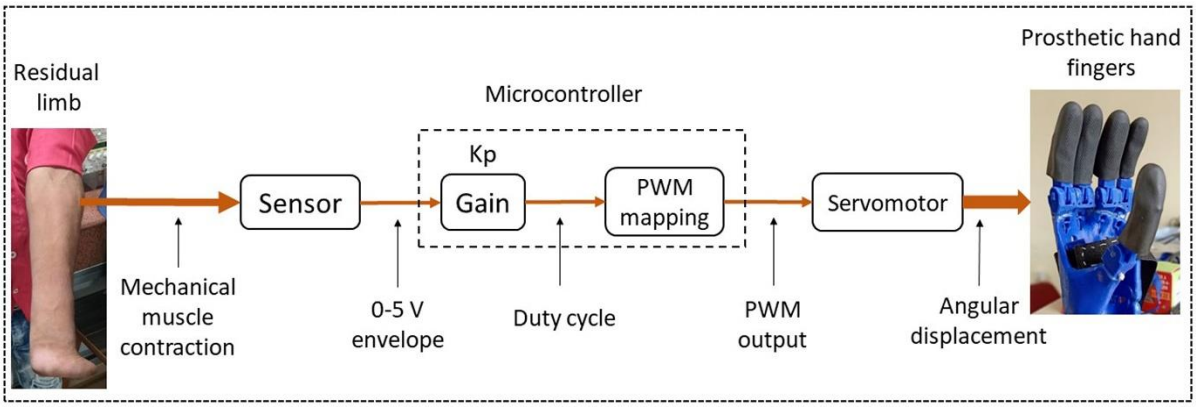

Figure 6.9 The control scheme for driving hand prototype.

6.4.2 Complete hand setup

The microcontroller unit with the implemented control scheme was integrated inside the hand prototype, which receives analog input from the FMG sensor and provides digital output to the servomotor. The sensor, actuator, and all electronic components receive a power supply from a 3.7 V, 2000 mAh rechargeable battery present within the hand. Figure 6.10 shows the complete hand setup prepared for left and right hand amputees. Silicon caps were installed at each finger to increase the grasping capability of the hand. The hand socket assembly consists of velcro strap for attaching it with the residual stump. A single pole single throw (SPST) switch was also incorporated inside the hand to power the whole hand setup (including the sensor). The hand offered a total of two degrees of freedom (DOF), and its overall weight was 350g. The maximum grip force measured at the fingertip using a dynamometer was 30 N. The hand setup was completely a standalone version, which can be easily attached to the residual limb of transradial amputees.

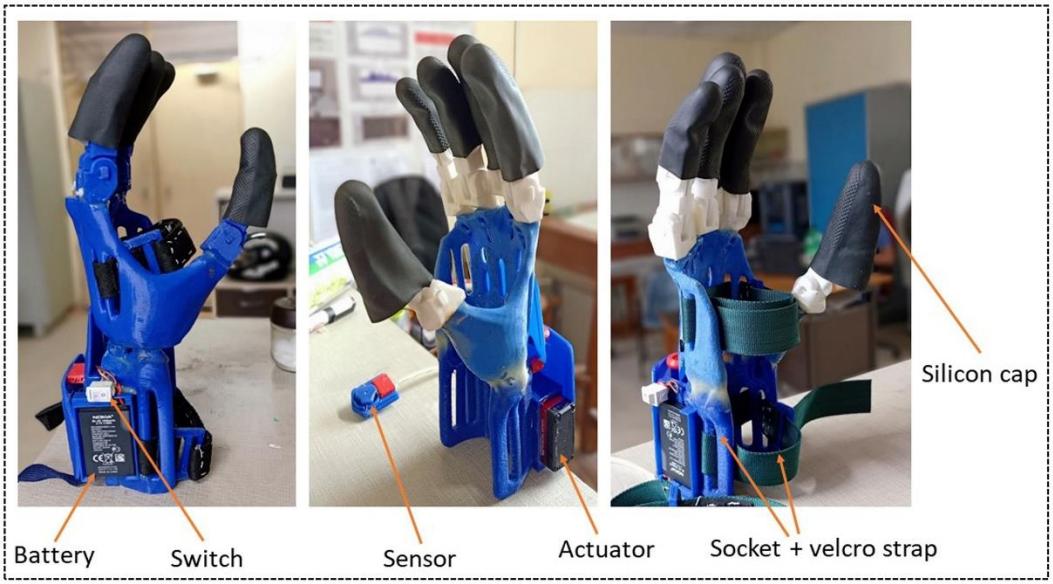

Figure 6.10 Developed hand prototype showing different parts.

6.4.3 Hand trial on amputees

The developed hand setup was effectively tested on three different subjects with below elbow amputations. Ethical approval was taken from the ethical committee, institute of medical sciences, BHU, Varanasi, before performing this trial. The hand prototype and the designed sensor were attached to the residual forearm stump of the amputee by using the velcro strap, as shown in Figure 6.11. The sensor was positioned on the skin in conjunction with the flexor carpi ulnaris muscle as these muscles on the forearm are accountable for the flexion and extension of fingers and wrist (Lobo-Prat et al. 2014; Supuk, Skelin, and Cic 2014).

The amputees wearing the hand prosthesis performed several activities such as grasping distinct objects, drinking water, opening the bottle, picking delicate items, etc. The implemented control scheme allowed amputees to proportionally actuate the hand fingers as per the intensity of captured FMG signals. Fig 6.12 describes the several tasks accomplished by an amputee wearing the developed prosthetic hand. Each amputee wore the prosthesis for four hours a day, and there was no report of muscle fatigue.

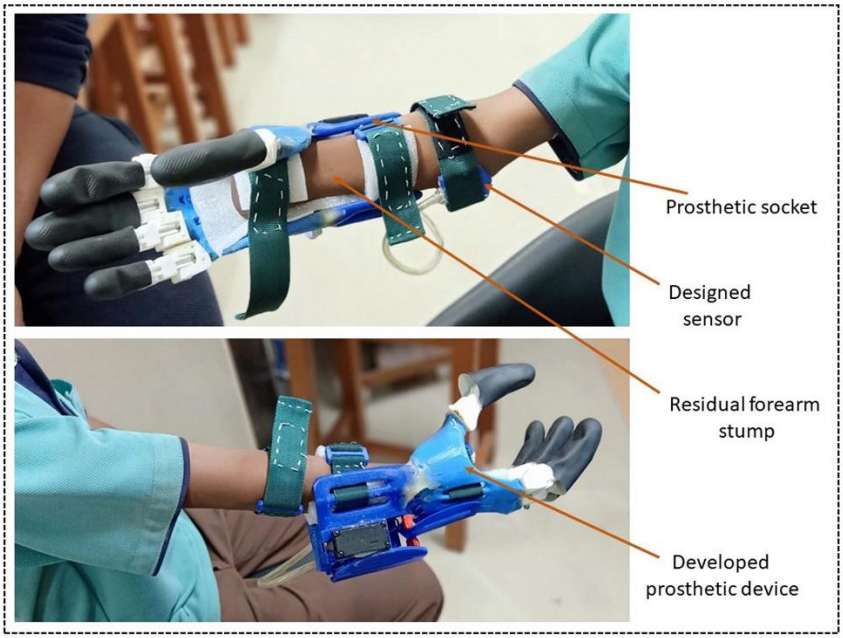

Figure 6.11 Attachment of developed prosthetic hand setup to the residual limb of an amputee.

Figure 6.12 Activities performed by an amputee wearing the developed hand.

Further, a full closing/opening time of the prosthetic hand was calculated from the recorded video to know the operating speed of the hand. The hand offered closing/opening time of 350/300 ms, which is comparable to that of ottobock sensor hand (having 300/300 ms), which is considered as the fastest available hand in the market (“Myoelectric Speed Hands”).

6.5 Conclusion

This chapter presents an affordable force myography controlled prosthetic hand for below-elbow amputees. A novel sensor was fabricated for extracting detailed information about the muscle contraction from the remaining upper-limb of amputees. The designed sensor with unique mechanical assembly and translating circuitry offers quantifiable and faithful detection of muscular contractions than the simple force sensors. A fully functional hand prosthesis was developed with a proportional control scheme that utilizes FMG signals from the sensor for its operation.

The sensor's performance was validated by determining its static and dynamic characteristics. The sensor showed a perfect similarity with the EMG sensor in detecting simultaneous muscle contractions. The sensor is also very less susceptible to noise as compared to an EMG sensor. These characteristics suggested the applicability of the designed sensor to control the prosthetic device as an alternative option to the EMG sensor. Moreover, the designed sensor also has other advantages such as does not require the use of electrodes and complex preprocessing units, easily wearable, low-cost, produces steady output, not sensitive to sweat or moisture, not affected by motion artifacts, etc. However, to get a reliable and repeatable output from the sensor, it's positioning on the sensitive portion of the skin (muscle) must be done discreetly.

The developed hand prototype, along with the designed FMG sensor, was tested on amputees for performing some necessary activities of daily life. The subjects utilizing their intention (of muscular contractions) were able to control the flexion of fingers for grasping objects. The sensor generated control was able to deliver faster and intuitive operation of the hand.

Parameters	Developed hand	Ottobock sensor hand
Mass	350 g	460 g
Material	Polylactic acid (PLA)	Silicone
Fabrication technique	3D printing (FDM)	Molding
Size	175x85x35 mm	184x80x40 mm
DOF	2	1
Number of actuators	2	1
Actuation method	Dc motor-tendons	Dc motor-worm gear
Control scheme	Proportional	Proportional
Feedback	no	force
Full closing time (response time)	350 ms	300 ms
Battery	3.7 V, Lithium-polymer, 2000 mAh	7.2 V, Lithium-ion, 2200 mAh
Sensor	Designed FMG sensor	EMG sensor
Price in the commercial market	Prototyping cost ($50)	$42000

Table 6.2 Comparison of developed hand with a commercial hand.

The comparison of a developed hand prototype with a commercial hand in terms of some important features is provided in Table 6.2. Compared to the commercial hand, the developed prototype offers almost similar features; the only difference is the absence of feedback. For future work, the feedback mechanism by using tactile sensors can be added to the hand to further enhance its grasping ability. One of the disadvantages with the hand is its limited functionality, which can be improved by developing a hand with multi DOF and implementing a classification based control scheme that receives signals from the designed sensor array.

Moreover, such a low-cost hand prosthesis controlled by the FMG signals can fulfill the basic needs of transradial amputees.

6.6 References

Abdoli-Eramaki, Mohammad, Caroline Damecour, John Christenson, and Joan Stevenson. 2012. "The Effect of Perspiration on the SEMG Amplitude and Power Spectrum." *Journal of Electromyography and Kinesiology* 22 (6): 908–13. https://doi.org/10.1016/j.jelekin.2012.04.009.

Agostini, V., and M. Knaflitz. 2012. "An Algorithm for the Estimation of the Signal-To-Noise Ratio in Surface Myoelectric Signals Generated During Cyclic Movements." *IEEE Transactions on Biomedical Engineering* 59 (1): 219–25. https://doi.org/10.1109/TBME.2011.2170687.

Ahsan, M. R., M. I. Ibrahimy, and O. O. Khalifa. 2011. "Hand Motion Detection from EMG Signals by Using ANN Based Classifier for Human Computer Interaction." In *Simulation and Applied Optimization 2011 Fourth International Conference on Modeling*, 1–6. https://doi.org/10.1109/ICMSAO.2011.5775536.

Amft, O., H. Junker, P. Lukowicz, G. Troster, and C. Schuster. 2006. "Sensing Muscle Activities with Body-Worn Sensors." In *International Workshop on Wearable and Implantable Body Sensor Networks (BSN'06)*, 4 pp. – 141. https://doi.org/10.1109/BSN.2006.48.

Asghari Oskoei, Mohammadreza, and Huosheng Hu. 2007. "Myoelectric Control Systems—A Survey." *Biomedical Signal Processing and Control* 2 (4): 275–94. https://doi.org/10.1016/j.bspc.2007.07.009.

"Bebionic Hand." Accessed October 21, 2019. https://www.ottobockus.com/prosthetics/upper-limb-prosthetics/solution-overview/bebionic-hand/.

Castellini, Claudio, Panagiotis Artemiadis, Michael Wininger, Arash Ajoudani, Merkur Alimusaj, Antonio Bicchi, Barbara Caputo, et al. 2014. "Proceedings of the First Workshop on Peripheral Machine Interfaces: Going beyond Traditional Surface Electromyography." *Frontiers in Neurorobotics* 8. https://doi.org/10.3389/fnbot.2014.00022.

Cho, Erina, Richard Chen, Lukas-Karim Merhi, Zhen Xiao, Brittany Pousett, and Carlo Menon. 2016. "Force Myography to Control Robotic Upper Extremity Prostheses: A Feasibility Study." *Frontiers in Bioengineering and Biotechnology* 4 (March). https://doi.org/10.3389/fbioe.2016.00018.

Connan, Mathilde, Eduardo Ruiz Ramírez, Bernhard Vodermayer, and Claudio Castellini. 2016. "Assessment of a Wearable Force- and Electromyography Device and Comparison of the Related Signals for Myocontrol." *Frontiers in Neurorobotics* 10 (November). https://doi.org/10.3389/fnbot.2016.00017.

Esposito, Daniele, Emilio Andreozzi, Antonio Fratini, Gaetano D Gargiulo, Sergio Savino, Vincenzo Niola, and Paolo Bifulco. 2018a. "A Piezoresistive Sensor to Measure Muscle Contraction and Mechanomyography." *Sensors (Basel, Switzerland)* 18 (8). https://doi.org/10.3390/s18082553.

Esposito, Daniele, Emilio Andreozzi, Antonio Fratini, Gaetano D Gargiulo, Sergio Savino, Vincenzo Niola, and Paolo Bifulco. 2018. "A Piezoresistive Sensor to Measure Muscle Contraction and Mechanomyography." Sensors (Basel, Switzerland) 18 (8). https://doi.org/10.3390/s18082553.

Fahrenkopf, Matthew P., Nicholas S. Adams, John P. Kelpin, and Viet H. Do. 2018. “Hand Amputations.” *Eplasty* 18 (September). https://www.ncbi.nlm.nih.gov/pmc/articles/PMC6173827/.

“FSR Integration Guide - Interlink Electronics | DigiKey.” Accessed June 15, 2019. https://www.digikey.com/en/pdf/i/interlink-electronics/interlink-electronics-fsr-force-sensing-resistors-integration-guide.

Ha, Nguon, Gaminda Pankaja Withanachchi, and Yimesker Yihun. 2018. “Force Myography Signal-Based Hand Gesture Classification for the Implementation of Real-Time Control System to a Prosthetic Hand.” In . American Society of Mechanical Engineers Digital Collection. https://doi.org/10.1115/DMD2018-6937.

Ha, N., Withanachchi, G.P. and Yihun, Y., 2019. “Performance of Forearm FMG for Estimating Hand Gestures and Prosthetic Hand Control.” *Journal of Bionic Engineering* 16 (1): 88–98. https://doi.org/10.1007/s42235-019-0009-4.

Hamner, Samuel R., Vinesh G. Narayan, and Krista M. Donaldson. 2013. “Designing for Scale: Development of the ReMotion Knee for Global Emerging Markets.” *Annals of Biomedical Engineering* 41 (9): 1851–59. https://doi.org/10.1007/s10439-013-0792-8.

Ibitoye, Morufu Olusola, Nur Azah Hamzaid, Jorge M. Zuniga, and Ahmad Khairi Abdul Wahab. 2014. “Mechanomyography and Muscle Function Assessment: A Review of Current State and Prospects.” *Clinical Biomechanics* 29 (6): 691–704. https://doi.org/10.1016/j.clinbiomech.2014.04.003.

“I-Limb Quantum | Touch Bionics.” Accessed April 12, 2019. http://touchbionics.com/products/active-prostheses/i-limb-quantum.

Junker, Holger, Oliver Amft, Paul Lukowicz, and Gerhard Tröster. 2008. “Gesture Spotting with Body-Worn Inertial Sensors to Detect User Activities.” *Pattern Recognition* 41 (6): 2010–24. https://doi.org/10.1016/j.patcog.2007.11.016.

Kannenberg, Andreas. 2017. “Active Upper-Limb Prostheses: The International Perspective.” *JPO: Journal of Prosthetics and Orthotics* 29 (4S): P57. https://doi.org/10.1097/JPO.0000000000000158.

Lobo-Prat, Joan, Peter N Kooren, Arno HA Stienen, Just L Herder, Bart FJM Koopman, and Peter H Veltink. 2014. “Non-Invasive Control Interfaces for Intention Detection in Active Movement-Assistive Devices.” *Journal of NeuroEngineering and Rehabilitation* 11 (1): 168. https://doi.org/10.1186/1743-0003-11-168.

Lukowicz, Paul, Friedrich Hanser, Christoph Szubski, and Wolfgang Schobersberger. 2006. “Detecting and Interpreting Muscle Activity with Wearable Force Sensors.” In *Pervasive Computing*, edited by Kenneth P. Fishkin, Bernt Schiele, Paddy Nixon, and Aaron Quigley, 3968:101–16. Berlin, Heidelberg: Springer Berlin Heidelberg. https://doi.org/10.1007/11748625_7.

Maduri, Prathusha, and Hossein Akhondi. 2020. “Upper Limb Amputation.” In *StatPearls*. Treasure Island (FL): StatPearls Publishing. http://www.ncbi.nlm.nih.gov/books/NBK540962/.

Matute, Arnaldo, Leonel Paredes-Madrid, Gelman Moreno, Fabián Cárdenas, and Carlos A. Palacio. 2018. “A Novel and Inexpensive Approach for Force Sensing Based on FSR Piezocapacitance Aimed at Hysteresis Error Reduction.” Research article. Journal of Sensors. 2018. https://doi.org/10.1155/2018/6561901.

Melocchi, Alice, Federico Parietti, Giulia Loreti, Alessandra Maroni, Andrea Gazzaniga, and Lucia Zema. 2015. “3D Printing by Fused Deposition Modeling (FDM) of a

Swellable/Erodible Capsular Device for Oral Pulsatile Release of Drugs." *Journal of Drug Delivery Science and Technology*, In Honor of Prof. Dominique Duchêne, 30 (December): 360–67. https://doi.org/10.1016/j.jddst.2015.07.016.

"Michelangelo Prosthetic Hand." Accessed April 12, 2019. https://www.ottobockus.com/prosthetics/upper-limb-prosthetics/solution-overview/michelangelo-prosthetic-hand/.

"Myoelectric Speed Hands." Accessed April 12, 2019. https://www.ottobockus.com/prosthetics/upper-limb-prosthetics/solution-overview/myoelectric-devices-speedhands/.

Pancholi, S., and A. M. Joshi. 2018. "Portable EMG Data Acquisition Module for Upper Limb Prosthesis Application." *IEEE Sensors Journal* 18 (8): 3436–43. https://doi.org/10.1109/JSEN.2018.2809458.

Paredes-Madrid, Leonel, Johanna Fonseca, Arnaldo Matute, Elkin I. Gutiérrez Velásquez, and Carlos A. Palacio. 2018. "Self-Compensated Driving Circuit for Reducing Drift and Hysteresis in Force Sensing Resistors." *Electronics* 7 (8): 146. https://doi.org/10.3390/electronics7080146.

Parker, P., K. Englehart, and B. Hudgins. 2006. "Myoelectric Signal Processing for Control of Powered Limb Prostheses." *Journal of Electromyography and Kinesiology: Official Journal of the International Society of Electrophysiological Kinesiology* 16 (6): 541–48. https://doi.org/10.1016/j.jelekin.2006.08.006.

Peerdeman, Bart, Daphne Boere, Heidi Witteveen, Rianne Huis in `tVeld, Hermie Hermens, Stefano Stramigioli, Hans Rietman, Peter Veltink, and Sarthak Misra. 2011. "Myoelectric Forearm Prostheses: State of the Art from a User-Centered Perspective." *The Journal of Rehabilitation Research and Development* 48 (6): 719. https://doi.org/10.1682/JRRD.2010.08.0161.

Phillips, Sam L., and William Craelius. 2005. "Residual Kinetic Imaging: A Versatile Interface for Prosthetic Control." *Robotica* 23 (3): 277–82. https://doi.org/10.1017/S0263574704001298.

Pylatiuk, Christian, Stefan Schulz, Artem Kargov, and Georg Bretthauer. 2004. "Two Multiarticulated Hydraulic Hand Prostheses." *Artificial Organs* 28 (11): 980–86. https://doi.org/10.1111/j.1525-1594.2004.00014.x.

Radmand, Ashkan, Erik Scheme, and Kevin Englehart. 2016. "High-Density Force Myography: A Possible Alternative for Upper-Limb Prosthetic Control." *Journal of Rehabilitation Research and Development* 53 (4): 443–56. https://doi.org/10.1682/JRRD.2015.03.0041.

Ravindra, Vikram, and Claudio Castellini. 2014. "A Comparative Analysis of Three Non-Invasive Human-Machine Interfaces for the Disabled." *Frontiers in Neurorobotics* 8. https://doi.org/10.3389/fnbot.2014.00024.

Sinderby, C., L. Lindström, and A. E. Grassino. 1995. "Automatic Assessment of Electromyogram Quality." *Journal of Applied Physiology (Bethesda, Md.: 1985)* 79 (5): 1803–15. https://doi.org/10.1152/jappl.1995.79.5.1803.

Slade, Patrick, Aadeel Akhtar, Mary Nguyen, and Timothy Bretl. 2015. "Tact: Design and Performance of an Open-Source, Affordable, Myoelectric Prosthetic Hand." In *2015 IEEE International Conference on Robotics and Automation (ICRA)*, 6451–56. Seattle, WA, USA: IEEE. https://doi.org/10.1109/ICRA.2015.7140105.

Supuk, Tamara Grujic, Ana Kuzmanic Skelin, and Maja Cic. 2014. “Design, Development and Testing of a Low-Cost SEMG System and Its Use in Recording Muscle Activity in Human Gait.” *Sensors (Basel, Switzerland)* 14 (5): 8235–58. https://doi.org/10.3390/s140508235.

Tavakoli, Mahmoud, Carlo Benussi, and Joao Luis Lourenco. 2017. “Single Channel Surface EMG Control of Advanced Prosthetic Hands.” *Expert Syst. Appl.* 79 (C): 322–332. https://doi.org/10.1016/j.eswa.2017.03.012.

Uellendahl, Jack. 2017. “Myoelectric versus Body-Powered Upper-Limb Prostheses: A Clinical Perspective.” *JPO: Journal of Prosthetics and Orthotics* 29 (4S): P25. https://doi.org/10.1097/JPO.0000000000000151.

“VINCENTevolution 3.” Accessed April 12, 2019. https://vincentsystems.de/en/prosthetics/vincent-evolution-3/.

Wang, Fang, Mohammadreza Asghari Oskoei, and osheng Hu. 2017. “Multi-Finger Myoelectric Signals for Controlling a Virtual Robotic Prosthetic Hand.” *International Journal of Modelling, Identification and Control* 27 (3): 181. https://doi.org/10.1504/IJMIC.2017.083780.

Williams, Matthew R, and Wayne Walter. 2015. “Development of a Prototype Over-Actuated Biomimetic Prosthetic Hand.” *PLOS ONE*, 15.

World Health Organization, 2011. World report on disability 2011. World Health Organization.

Xiao, Zhen G, and Carlo Menon. 2014. “Towards the Development of a Wearable Feedback System for Monitoring the Activities of the Upper-Extremities.” *Journal of NeuroEngineering and Rehabilitation* 11 (1): 2. https://doi.org/10.1186/1743-0003-11-2.